Journal Pre-proof

Performance enhancement of CIGS thin-film solar cell

Mohamed Wahid Bouabdelli, Fatiha Rogti, Mostefa Maache, Abdelaziz Rabehi

Please cite this article as: Bouabdelli MW, Rogti F, Maache M, Rabehi A, Performance enhancement of CIGS thin-film solar cell, *Optik* (2020), doi: https://doi.org/10.1016/j.ijleo.2020.164948

This is a PDF file of an article that has undergone enhancements after acceptance, such as the addition of a cover page and metadata, and formatting for readability, but it is not yet the definitive version of record. This version will undergo additional copyediting, typesetting and review before it is published in its final form, but we are providing this version to give early visibility of the article. Please note that, during the production process, errors may be discovered which could affect the content, and all legal disclaimers that apply to the journal pertain.

Performance enhancement of CIGS thin-film solar cell

Mohamed Wahid Bouabdelli[1], Fatiha Rogti[1], Mostefa Maache[2], Abdelaziz Rabehi[3,4].

[1] Laboratoire d'Analyse et de Commande des Systèmes d'Energie et Réseaux électriques, Faculté de Technologie, Université Amar Telidji de Laghouat, BP 37G, Route de Ghardaïa, 03000 Laghouat, Algeria

[2] Department of Physics, FECS, Ziane Achour University, 17000 Djelfa, Algeria

[3]Département d'électronique, Institue des sciences et des technologies, Centre universitaire de Tissemsilt, 38000,Algeria

[4]Laboratoire de Micro-électronique Appliquée. Université Djillali Liabès de Sidi Bel Abbés, BP 89, 22000, Sidi Bel Abbés, Algeria

ABSTRACT

In the present study, A thin-film solar cell based on Cu(In,Ga)Se$_2$ (CIGS) is carried out using two-dimensional device simulator called Silvaco–Atlas. A basic CIGS solar cell was simulated under the room temperature of 298 k. It is found that the obtained simulation results agree very well with recent published experimental results, which validate our used model. The aim of this study is to enhance the CIGS solar cell performance by optimizing its parameters. For this purpose, the CIGS cell layer thicknesses and doping densities have been optimized. With this optimization process, the cell efficiency increases from 22.9 to 27.5 %. In several research studies, the CIGS solar cells were tested under the room temperature but the realistic operating temperature is varied. In order to optimize the operating temperature and study its effect on the CIGS cell performance, the operating temperature was varied. The results show that as the temperature decreases, the cell performance increases. At the optimum temperature of 240 k, the CIGS cell achieves a very important efficiency of 32.45 %.

Keywords: CIGS solar cell, Silvaco–Atlas, temperature, optimization, performance.

1. INTRODUCTION

The growing demand for energy and the negative effects of traditional energy sources (fossil fuels) on the environment require us to look for variable sources of sustainable and clean energy that can be a promising alternative to traditional energy. The solar is the most important source of renewable and clean energy, study on solar cells is a major area of interest within the field of energy .Many materials have been developed to produce thin film solar cells such as CdTe, CIGS and CZTS. The CIGS (Copper-Indium-Gallium-diSelenide) based solar cell is considered as one of the most promising thin film solar cell due to its many features such as higher efficiency both on module and cell levels [1], simple processes of manufacturing [2,3], low cost production [2], excellent durability and stability [4] radiation hardness [5]. In addition, the CIGS solar cells have other attractive options for consumers such as flexibility and lightweight [6, 7]. The CIGS material has a very high absorption coefficient in the order of 10^5 cm^{-1} in the visible sunlight spectrum [3, 8]. The Cu(In$_{(1-x)}$,Ga$_x$)Se$_2$ (CIGS) alloys is quaternary compound semiconductor with a chalcopyrite structure [2, 9], where $x=Ga/(Ga+In)$ is the mole fraction of Ga (Ga-content). The CIGS has a direct bandgap adjustable with x. By varying x from 0 to 1, the CIGS band gaps varies from 1.04 eV to 1.68 eV [10, 11, 12].

The main current challenge in the photovoltaic field is to improving the solar cell performance. Several photovoltaic research centers and companies have improved experimentally the CIGS solar cell efficiency. In the last few years, the single junction CIGS based solar cells showed increasing record efficiencies of 19.9 % in NREL (National Renewable Energy Laboratory) [13], 20.4 % in Empa (Swiss Federal Laboratories for Materials Science and Technology) [14], 21.0 % in Solibro [15], 22.6 % in ZSW (the Center of Solar Energy and Hydrogen Research) [16]. Finally, SF (Solar Frontier K.K.) achieved the current record efficiency of 22.9 % for CdS/CIGS based solar cell. [1, 17, 18]. Furthermore, many theoretical and simulation studies investigated the CIGS solar cell in order to enhance its performance such as the studies that are found in literatures [19-26].

In order to enhance greatly the CIGS solar cell performance, all most important parameters that affect cell performance are optimized in this study. The thickness and doping density are important parameters for improving the cell performance and reducing the cell cost production. Temperature is other very important parameter that determining the photovoltaic cell features. Furthermore, in several research studies, the operating temperature for

solar cell was 25 °C (298 k) [1]. However, in realistic scenarios, the operating temperatures are varied due to installing photovoltaic panels in different regions. Thus, studying the CIGS solar cell performance in variable temperatures is very necessary. For this reason, the CIGS solar cell is tested here under variable temperatures between 240 to 400k.

The purpose of this study is to enhance the performance of CIGS based solar cell and particularly exceed the record efficiency of 22.9 % [18]. For these purposes, we have optimized the temperature, the layer thicknesses and doping densities of the CIGS cell using Atlas-Silvaco numerical simulation program. We first report the design of CIGS solar based on previous studies and validate our model by comparing it with the previous experimental and simulation models. Secondly, we optimize the layer thicknesses and doping densities and determine its optimum values. By combining the optimum parameters, the optimized cell has been designed and its results are compared with those of the basic cell. Then, we optimize the cell temperature and study its effects on cell performance. Finally, all the results are summarized as a conclusion.

2. NUMERICAL MODEL DESCRIPTION

The modeling and Physically-based simulation has become a very important tool in understanding device operation and physical mechanisms because the simulation processes are more available, cheaper and faster than experimental performing and it can provide information that is difficult or impossible to measure experimentally.

Atlas–Silvaco is a two- (2D) and three-dimensional (3D) powerful device simulator and worldwide support in analyzing and optimizing the performance of semiconductor devises. It provides a large variety of physical and mathematical models and appropriate mesh structure .It make reliable predictions and accurately characterization of the electrical, optical and thermal behaviors of current and new semiconductor devices such as the solar cells [26]. Atlas–Silvaco is used in this study to modeling and optimizing single junction CIGS solar cell, which are conducted by solving coupled system of the basic semiconductor equations. The used numerical method is the Newton method, the main basic semiconductor equations are the continuity equations and the Poisson equation. The following expressions that describe the main basic semiconductor equations and the performance parameters are obtained from the literature [2, 27, 28, 29]:

The Poisson equation is given by:

$$\Delta V = -\frac{q}{\varepsilon}\left[p - n + N_D - N_A + N_t \right] \tag{1}$$

Where V is the electrostatic potential, q is an electron charge, ε is the permittivity, N_A is the acceptor doping density, N_D is the donor doping density, p is the hole density, n is the electron density and N_t is the acceptor-type and donor-type defect density. The continuity equations for electrons and holes are obtained by:

$$-\frac{1}{q}\frac{dJ_n}{dx} = G_{op}(x) - R_n \tag{2}$$

$$\frac{1}{q}\frac{dJ_p}{dx} = G_{op}(x) - R_p \tag{3}$$

Where J_p is the hole current density, J_n is the electron current density, R_p is the hole recombination rate and R_n is the electron recombination rate, G_{op} is the optical generation rate. The recombination rates are modeled by the Shockley-Read-Hall (SRH) model as:

$$R_{n,p} = \frac{\sigma_n \sigma_p v_{th} N_t (np - n_i^2)}{\sigma_n\left[n + n_i \exp(\frac{E_t - E_i}{kT}) \right] + \sigma_p\left[p + n_i \exp(\frac{E_t - E_i}{kT}) \right]} \tag{4}$$

Where n_i is the intrinsic carrier density, k is Boltzmann constant, T is temperature, v_{th} is the thermal velocity, σ_n is the electron capture cross section, σ_p is the hole capture cross section, E_i is the intrinsic Fermi energy level, E_t is the trap energy level. The photogeneration rate G_{op} is given by:

$$G_{op}(x) = \frac{P_{in}\left(1 - r\right)\alpha}{AE_{ph}} \exp(-\alpha x) \tag{5}$$

Where E_{ph} is a photon energy, α is the absorption coefficient, r is the surface reflection, P_{in} is the incident optical power and A is the illuminated device area.

The current-voltage (J-V) equation of the solar cell is a sum of the photocurrent I_{ph} and the dark current, it is obtained by the celebrated Shockley equation:

$$I = I_{ph} - I_0\left(\exp(\frac{qV}{akT}) - 1 \right) \tag{6}$$

The main performance parameters of the solar cell are defined as follows:

The short-circuit current is expressed as:

$$I_{sc} = I_{ph} \tag{7}$$

The open-circuit voltage is given by:

$$V_{oc} = \frac{akT}{q}\ln(\frac{I_{ph}}{I_0}) \tag{8}$$

The open-circuit voltage also can be written as:

$$V_{oc} = \frac{E_g}{q} - \frac{akT}{q}\ln(\frac{I_{00}}{I_{ph}})$$

(9)

The fill factor FF is calculated by:

$$FF = \frac{P_{max}}{V_{oc}I_{sc}}$$

(10)

The cell efficiency η is given as:

$$\eta = \frac{P_{max}}{P_{in}} = \frac{V_{oc}I_{sc}FF}{P_{in}}$$

(11)

Where a is the ideality factor, P_{max} is the maximum power, I_{00} is saturation current prefactor and I_0 is the reverse saturation current. The approximate expression of the saturation reverse current I_o (for $w>>L$) is given by:

$$I_0 = q(\frac{D_n n_{i,p}{}^2}{L_n N_A} + \frac{D_p n_{i,n}{}^2}{L_p N_D})$$

(12)

Where $n_{i,p}$ and $n_{i,n}$ is the intrinsic carrier densities of p-doped and n-doped layers, D_p and D_n are the hole and electron diffusion coefficients, L_p and L_n are the hole and electron diffusion lengths respectively.

3. SOLAR CELL STRUCTURE AND MATERIALS PARAMETERS

The basic CIGS solar cell consists of a stack of layers deposited on substrate glass with an area of 1 cm^2. These layers from bottom to top are as follows: the Molybdenum back contact (0.5 μm), the p-doped Cu(In$_{(1-x)}$,Ga$_x$)Se$_2$ (2 μm) with x≈0.3 used as the absorber layer, the n-doped CdS (0.05 μm) as the buffer layer, the intrinsic (undoped) ZnO (0.05 μm) as second buffer layer and the n-doped ZnO layer (0.2 um) as window layer or transparent conducting oxide (TCO). This used structure is similar to the cell structures that were experimentally used in [16, 17]. The basic cell structure is displayed in figure 1.
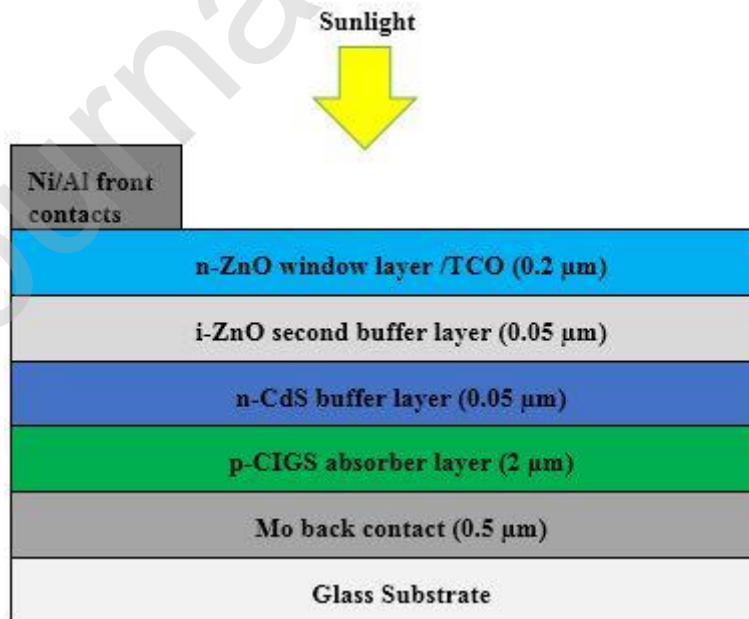
Figure 1. The basic cell structure

The following simulation parameters of all components of the solar cell are defined to be used as inputs for Silvaco-Atlas software. The CIGS solar cell has simulated under the standard test conditions (STC) that are: AM 1.5 G global solar spectrum, incident power density of 1000 W/m^2 and the room temperature of 25 °C [16, 17]. The Ga-content (x) of the CIGS (CuIn$_{1-x}$Ga$_x$Se$_2$) material is chosen to be around 0.3. The reported record efficiencies of CIGS solar cell have been achieved when x≈0.3 that is considered as the typical value of x [2, 13, 16, 30, 31]. The dependences of CIGS electrical and optical parameters on Ga-content (x≈0.3) are taken into account in determining of the following simulation parameters. The optical parameters are obtained from the experimental data found in [32], [33] and [34] for CIGS, CdS and ZnO respectively, the optical parameters of Molybdenum are available in the SOPRA database of the Silvaco-Atlas library. The electrical parameters of all materials are obtained from the literature [27, 35-37]. All CIGS cell layers contain many kinds of defects and impurities, the defect parameters determine the important recombination phenomenon in solar cell, the recombination phenomenon is modeled by Shockley-Read-Hall (SRH) model (equation. 4) that is implemented in Silvaco-Atlas [27]. The layer defect parameters are obtained from [30, 31, 35]. All defect and electrical parameters are presented in table 1.

Table 1. The defect and electrical parameters of CIGS solar cell layers

Parameters	p-CIGS	n-CdS	n-ZnO
Thickness w (μm)	2	0.1	0.2
Doping density (cm^{-3})	$N_A = 10^{15}$	$N_D = 10^{18}$	$N_D = 10^{18}$
Relative permittivity ε_r (F cm^{-1})	13.6	10	9
Band gap energy E_g (eV)	1.3	2.48	3.3
Electron affinity χ_e (eV)	4.58	4.18	4.5
Valence band effective density of states N_v (cm^{-3})	1.8×10^{19}	2.57×10^{19}	1.8×10^{19}
Conduction band effective density of states N_c (cm^{-3})	2.2×10^{18}	2.41×10^{18}	2.2×10^{18}
Electron mobility μ_n (cm^2/V s)	100	100	100
Hole mobility μ_p (cm^2/V s)	25	25	25
Defect type	Donor	Acceptor	Donor
Defect density N_t (cm^{-3})	10^{14}	10^{18}	10^{17}
Defect energy position E_t (eV)	0.3	mid-gap*	mid-gap*
Electron capture cross section σ_n (cm^2)	10^{-13}	10^{-17}	10^{-12}
Hole capture cross section σ_p (cm^2)	10^{-15}	10^{-12}	10^{-15}

* mid-gap is the middle of the band gap

4. RESULTS AND DISCUSSION

4.1. Simulation of the basic CIGS solar cell

The basic CIGS solar cell is simulated using the parameters listed in the previous table 1. The J-V (current-voltage) curve resulting from the simulation is shown in figure 2 and the performance parameters extracted from the corresponding J–V curve are listed in table 2. In order to validate our used model, the performance parameters of our simulated cell are compared with the performance parameters of the experimental record-efficiency cell taken from [17] and those of other simulated cell found in [20]. All results are listed in the table 2.
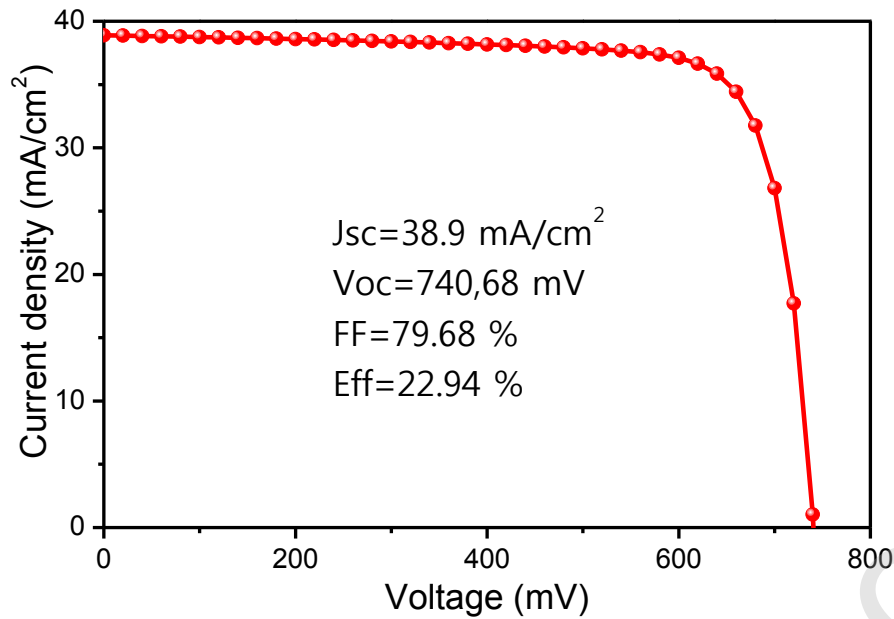
Figure 2. J-V curve of the basic CIGS solar cell.

Table 2 – Results of our simulated CIGS solar cell compared with other experimental and simulated results

Performance parameters	Our simulated cell (This work)	The experimental cell [17]	Other Simulated cell [20]
J_{SC} (mA/cm²)	38.9	38.5	34.866
V_{OC} (mV)	740.68	746	666
FF (%)	79.68	79.7	79.88
Efficiency η (%)	22.94	22.92	18.50

As shown in the table 2, it is evident that all the performance parameters of our simulated cell are very close to those of the experimental cell [17], and they are better than those of the simulated cell [20]. This good agreement between our results and the experimental results can validate the model and parameters used in this simulation and support the next simulation results.

4.2. Optimization of the CIGS solar cell parameters

The optimization of the CIGS solar cell parameters was conducted by varying the thickness and doping density of each layer of the CIGS solar cell and holding constants the other parameters, then determining the optimum thicknesses and doping densities that obtain the best cell performance.

4.2.1 Optimization of the CIGS absorber layer thickness and doping density

The CIGS layer thickness was varied from 1 to 10 μm and the CIGS layer doping density was varied from 10^{14} to 10^{17} cm^{-3} while all other parameters were stayed constant. Figures 3 and 4 display the main performance parameters such as the conversion efficiency (η), the fill factor (FF), the short circuit current density (J_{SC}) and the open circuit voltage (V_{OC}) versus the CIGS layer thickness and versus the CIGS layer doping density respectively.
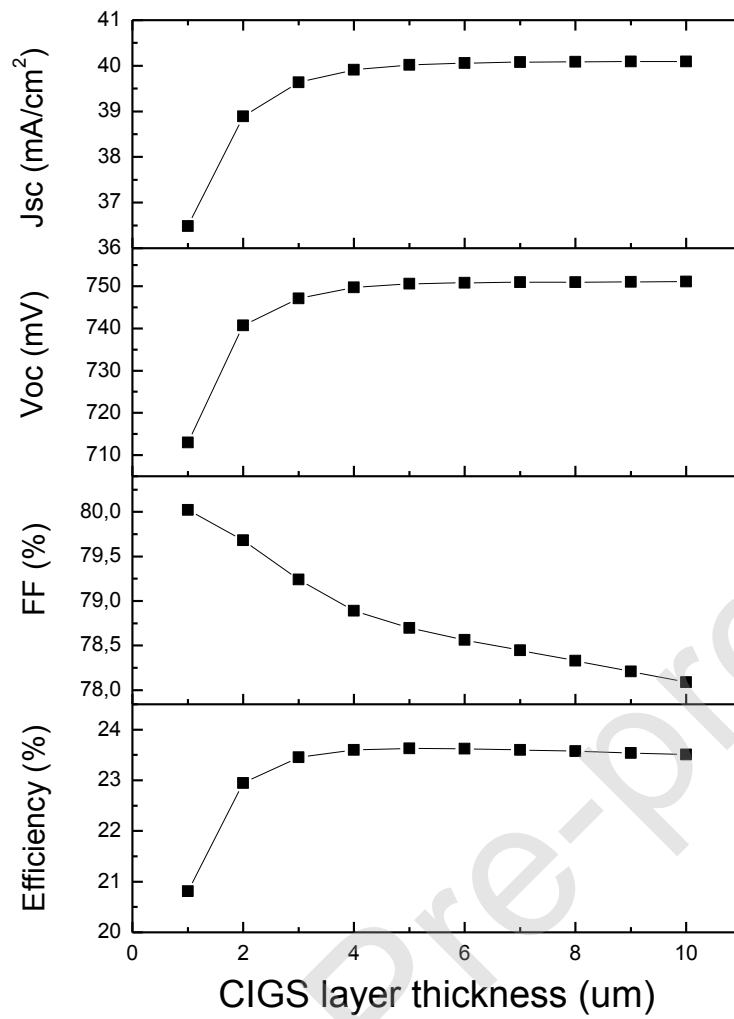
Figure 3. The cell performance parameters versus CIGS layer thickness
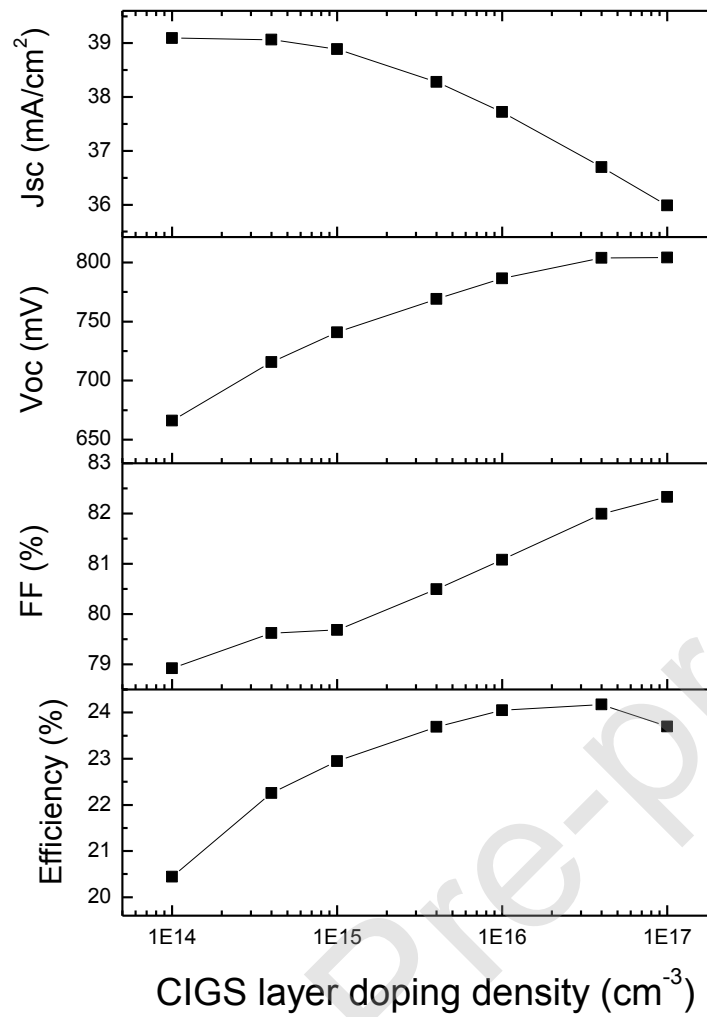
Figure 4. The cell performance parameters versus CIGS layer doping density N_A

Figure 3 shows that as the CIGS layer thickness increases from 1 to 5 µm, the efficiency η, V_{OC} and J_{SC} increase rapidly while the fill factor FF decreases. Beyond 5 µm thickness, the fill factor FF continues to decrease while the other performance parameters remains almost constant. Thus, the thickness of 5 µm is the optimal absorber layer thickness at which the efficiency reaches 23.89 %. Similar behaviors of the performance parameters were reported in [21, 22, 24]. These results can explained by the fact that as the CIGS thickness increases, more photons are absorbed. The absorbed photons generate more carriers (electron–hole pairs), which contribute to increasing photocurrent I_{ph} and thus increasing cell performance parameters that depend on the photocurrent according to Equations (7, 8, 10, 11). When the CIGS thickness continues to increase, it exceeds the diffusion length L_n. The light absorbed outside the diffusion length does not contribute to the photocurrent [28]. Thus, the cell performance remain constant.

Figure 4 shows that as the CIGS layer doping density increases from 10^{14} to 10^{17} cm^{-3},the short circuit current density J_{SC} shows a very slight decrease then it decreases because the increase in acceptor doping leads to decrease in the width of depletion region from which the major contribution to the photocurrent comes [28]. On the other hand, as the CIGS doping density increases from 10^{14} to 10^{17} cm^{-3}, the fill factor FF increases, the open circuit voltage Voc increases rapidly then it remains constants. This can be justified by the fact that the increase in doping density N_A decreases the saturation reverse current I_0, which increases Voc according to

Eq. 12 and Eq. 8. As the CIGS doping density increases from 10^{14} to 4×10^{16} cm^{-3}, the efficiency increases. Above 4×10^{16} cm^{-3} doping density, the efficiency decreases. The efficiency variation depends on both J_{SC} and Voc variation according to Eq. 11. The efficiency reaches a peak of 24.18 % at 4×10^{16} cm^{-3} which is the optimum CIGS layer doping density.

4.2.2 Optimization of the CdS buffer layer thickness and doping density

The CdS layer thickness was varied from 0.02 to 0.2 μm and the CdS layer doping density was varied from 10^{17} to 10^{22} cm^{-3} while all other parameters were remained constant. Figures 5 and 6 display the main performance versus the CdS layer thickness and versus the CdS layer doping density respectively.
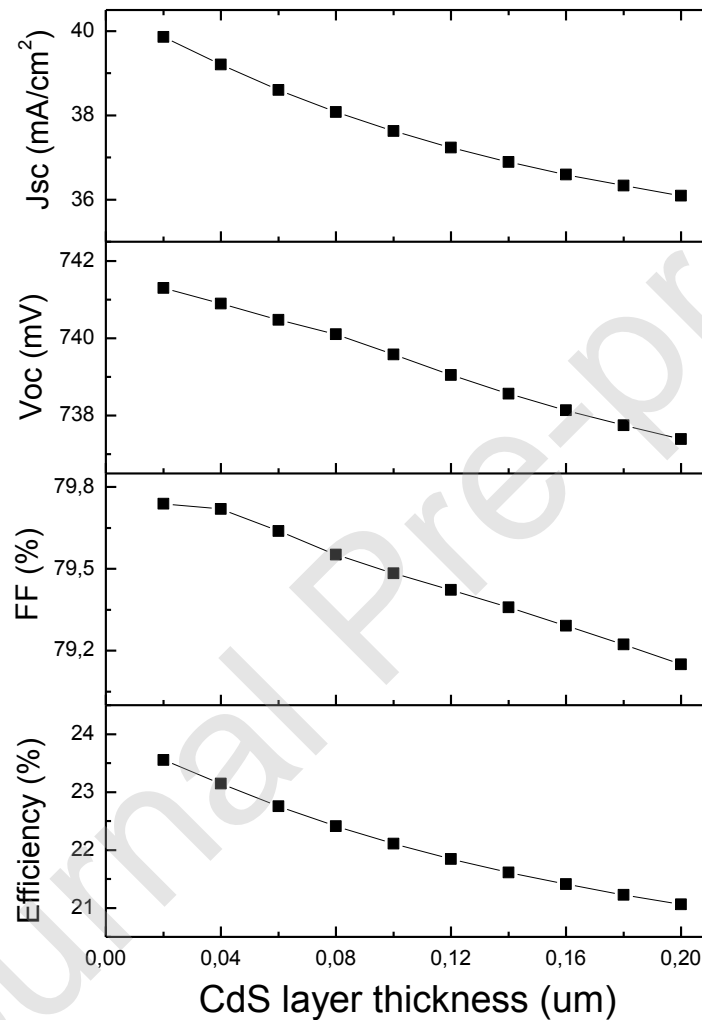

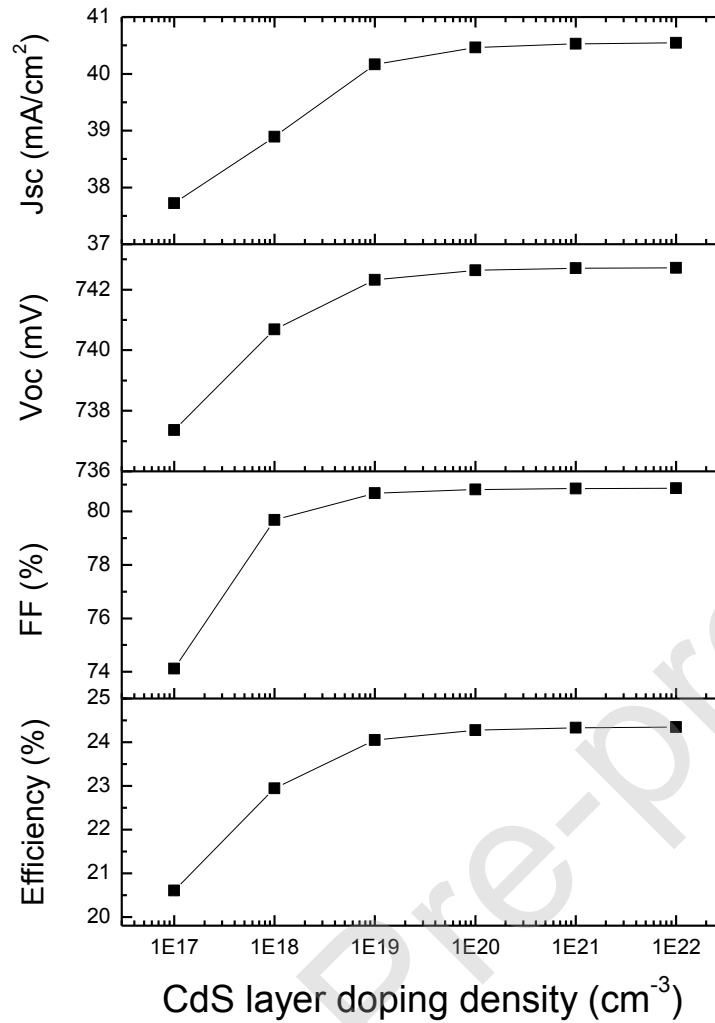**Figure 5.** The cell performance parameters versus CdS layer thickness

Journal Pre-proof

Figure 6. The cell performance parameters versus CdS layer doping density N_D

From Figure 5, as the CdS layer thickness increases from 0.02 to 0.2 µm, all performance parameters decrease. At 0.02 µm CdS thickness, the efficiency reaches the peak of 23.55 %. Thus, the thickness of 0.02 µm is the optimal CdS buffer layer thickness, which improves the cell performance and reduces the cell thickness. Similar trends of the performance parameters were demonstrated in [21, 22, 24]. These results can justified by the fact that as the CdS buffer thickness increases, the CdS absorbs more photons that can reach the absorber layer, which reduces the carrier generation in absorber layer. Thus, the photocurrent and the performance parameters decrease.

Figure 6 shows that as the CdS layer donor doping density increases from 10^{17} to 10^{20} cm^{-3}, all the cell performance parameters increase. Beyond 10^{20} cm^{-3} doping density, the performance parameters remains almost constant. Thus, the optimum CdS doping density is chosen to be 10^{20} cm^{-3} at which the efficiency reaches 24.28 %. These results can be explained by the fact that according to Eq. 12 and Eq. 8, as the acceptor doping density N_D increases, the saturation reverse current I_0 decreases, which increase the open circuit voltage V_{OC}, and thus the cell performance parameters.

4.2.3 Optimization of the n-ZnO window layer thickness and doping density

The n-ZnO layer thickness was varied from 0.02 to 0.32 μm while all other parameters were stayed constant. Figure 7 displays the main performance parameters versus the n-ZnO layer thickness.
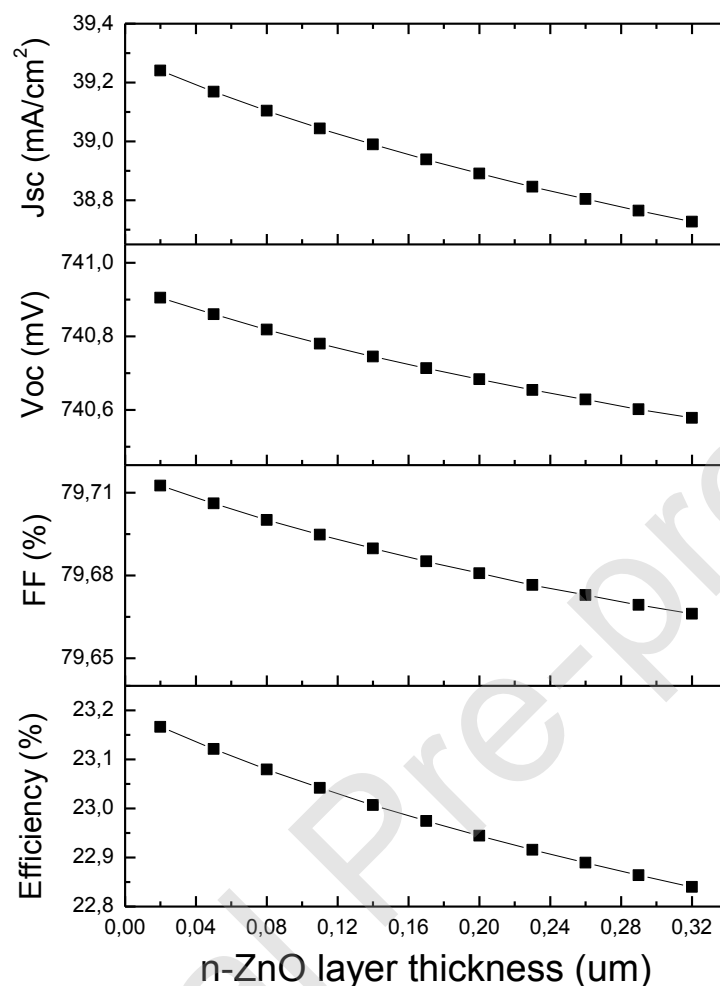

Figure 7. The cell performance parameters versus n-ZnO layer thickness

Figure 7 shows that as the n-ZnO layer thickness increases from 0.02 to 0.32 μm, all performance parameters decrease slightly. At 0.02 μm ZnO thickness the efficiency reaches the peak of 23.17 %. Thus, thickness of 0.02 μm is the optimal ZnO window layer thickness. Similarly to CdS, thick ZnO absorbs many photons that can reach the absorber layer which reduces the photogeneration and thus the cell performance parameters. Thick buffer and window layer affect negatively the cell performance because the light absorption of window and buffer layers cause optical losses in absorber layer and thus current losses. The CdS effect on cell performance is greater than ZnO due to the CdS optical absorption that is greater than ZnO absorption.

The n-ZnO doping density was varied between 10^{17} and 10^{22} cm^{-3} while the other while all other parameters were stayed unchanged. The results show that all cell performance parameters such as J_{SC}, V_{OC}, fill factor and efficiency remain almost constant when the ZnO doping density varies. This result can be justified by the fact that the window layer is located outside the PN junction. Thus, the effect of ZnO doping density on the depletion region width and thus the photocurrent is negligible.

4.2.4 The Optimized CIGS solar cell

An optimized cell was designed and simulated by combining the optimum layer thickness and doping density that are 5 µm and 4×10^{16} cm^{-3} for the CIGS absorber layer, 0.02 µm and 10^{20} cm^{-3} for the CdS buffer layer, 0.02 µm and 10^{18} cm^{-3} for the ZnO window layer respectively. The J-V curves for both the optimized cell and the basic cell are displayed in figure 8. The performance parameters of the optimized cell with those of the basic cell are presented in table 3.

Table 3: The performance parameters of the basic cell compared to those of the optimized cell.

Performance parameters	The basic cell	The optimized cell
J_{SC} (mA/cm^2)	38.9	39.75
V_{OC} (mV)	740.68	830.57
FF (%)	79.68	83.25
Efficiency η (%)	22.94	27.48

As shown in the table 3 and figure 8, it can be seen that the optimized cell shows improvement over the basic cell in performance parameters, which are significant improvements of 89.89 mV in V_{OC}, 3.57 % in fill factor FF 4.54 % in efficiency and a small improvement of 0.85 mA/cm^2 in J_{SC}.
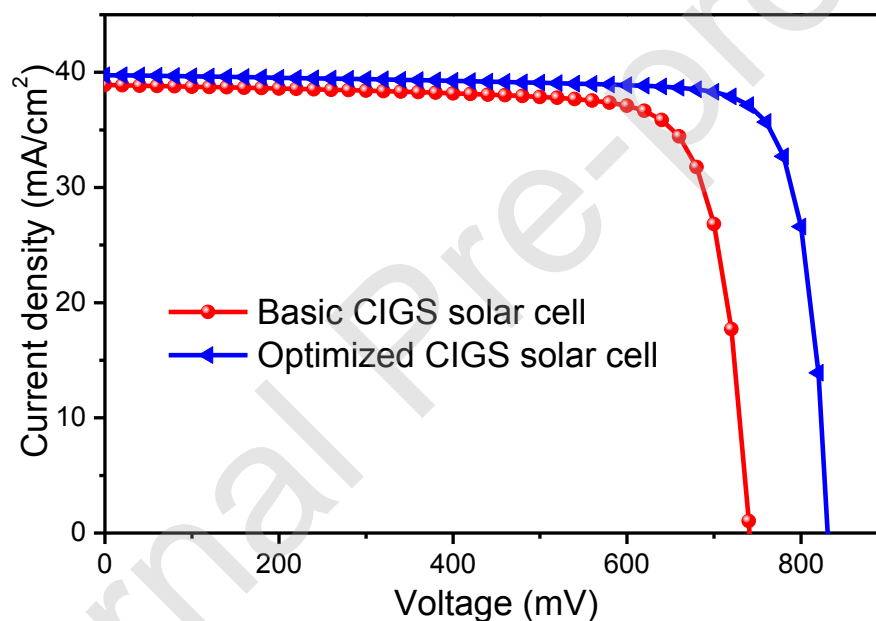

Figure 8: J-V curve for both the optimized cell and the basic cell

4.3. Effect of the operating temperature on the CIGS solar cell performance

After the optimization of the CIGS solar cell parameters, in order to study the effect of the temperature on the CIGS cell behaviors, the previous optimized cell was simulated under temperature varied from 240 K to 400 K. Figure 9 displays the main performance parameters versus the temperature variation.
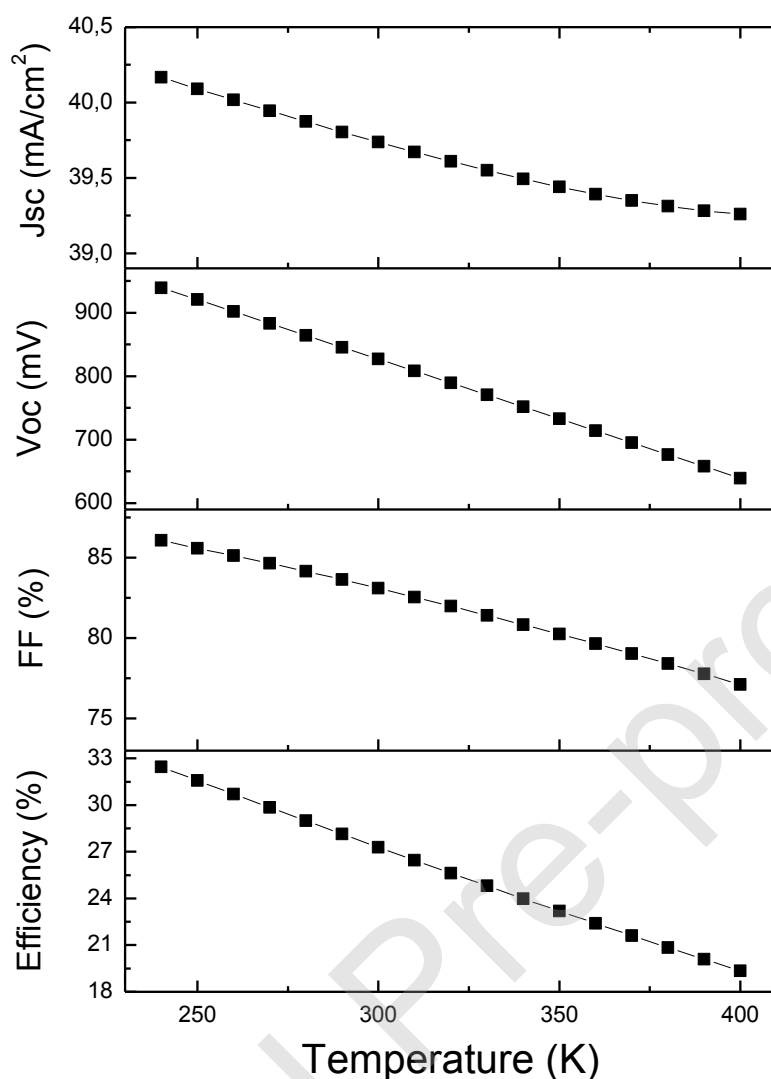
Figure 9. The cell performance parameters versus temperature

As shown in figure 9, the decrease in temperature affects positively and strongly the cell performance parameters. As temperature decreases, all performance parameters increase quasi-linearly, J_{SC} increases slightly while V_{OC}, FF and efficiency increase quickly. The increase in efficiency is around 0.8 % per 10 kelvin and 2 mV/K in V_{OC}. At 240 K temperature, the cell efficiency reach a peak of 32.45 %. Thus, 240k is the optimum temperature. Similar behaviours of performance parameters were reported in [20, 25]. The increase in the performance parameters is mainly due to the increase in V_{OC}. As temperature decreases, open circuit voltage V_{OC} linearly increases because of its linear dependence on temperature according to Eq. 9.

As a result, the temperature plays major factor that determining the CIGS solar cell performance, the decrease in temperature improves significantly the cell efficiency. Thus, it is desirable to decrease the cell temperature up to 240k. Decreasing the cell temperature is conducted by installing the cell on low temperature regions or by using PV cell cooling techniques. Different PV cell cooling techniques have been developed such as water cooling, forced air cooling, the PCM material... [38, 39]. For example, the use of PCM material can reduce the PV panel temperature by 35.6 k [39].

5. CONCLUSION

In conclusion, a basic CIGS solar cell was simulated under the room temperature of 298k. The simulation results are in good agreement with the experimental results. After optimization of the cell layer thicknesses and doping densities, it is found that the optimum layer thicknesses are 5 μm for CIGS absorber layer, and 0.02 μm for CdS buffer layers and ZnO window layer. The optimum layer doping densities are 4×10^{16} cm^{-3} for the CIGS absorber layer, 10^{20} cm^{-3} for the CdS buffer layer and 10^{18} cm^{-3} for the ZnO window layer. With these typical parameters, the optimized cell achieves an efficiency of 27.48 %. The temperature effect on CIGS cell performance has been analysed. The results show that the decrease in temperature enhances significantly the cell efficiency. At the optimum temperature of 240k, the cell efficiency reaches a peak value of 32.45 % that exceeding the record efficiency by a very significant improvement of 9.53 %. Thus, it is desirable to decreasing the cell temperature by installing the cell on low temperature regions or by using PV cell cooling techniques. The results of this simulation can be helpful for experimenters to fabricate CIGS solar cells with high efficiencies that increasing the current record efficiency.

Declaration of interests

The authors declare that they have no known competing financial interests or personal relationships that could have appeared to influence the work reported in this paper.

REFERENCES

[1] M. A. Green, Y. Hishikawa, E. D. Dunlop, D. H. Levi, J. Hohl-Ebinger, M. Yoshita, and A. W. Ho-Baillie, Solar cell efficiency tables (Version 53), Progress in Photovoltaics: Research and Applications 27 (2019) 3–12. https://doi.org/10.1002/pip.3102

[2] A. Luque and S. Hegedus (eds), Handbook of Photovoltaic Science and Engineering, 1st Ed, John Wiley & Sons Ltd, England, 2003. https://doi.org/10.1002/0470014008

[3] T. Kato, Cu(In,Ga)(Se,S)2 solar cell research in Solar Frontier: Progress and current status, Japanese Journal of Applied Physics 56 (2017) 04CA02. https://doi.org/10.7567/JJAP.56.04CA02

[4] H. S. Ullal, K. Zwelbel, and B. Von Roedern, Current status of polycrystalline thin-film PV technologies. Conference Record of the Twenty Sixth IEEE Photovoltaic Specialists Conference – 1997, IEEE (1997) 301-305. https://doi.org/10.1109/PVSC.1997.654089

[5] M. Yamaguchi, Radiation resistance of compound semiconductor solar cells, Journal of applied physics 78 (1995) 1476 - 1480. https://doi.org/10.1063/1.360236

[6] S. Ishizuka, A. Yamada, P. Fons, and S. Niki, Flexible Cu(In,Ga)Se2 solar cells fabricated using alkali-silicate glass thin layers as an alkali source material, Journal of Renewable Sustainable Energy 1 (2009) 013102. https://doi.org/10.1063/1.3005376

[7] A. Chirilă, S. Buecheler, F. Pianezzi, F. Bloesch, C. Gretener, A. R. Uhl, C. Fella, L. Kranz, J. Perrenoud, S. Seyrling, S. Verma, S. Nishiwaki, Y. E. Romanyuk, G. Bilger, and A. N.Tiwari, Highly efficient Cu(In,Ga)Se2 solar cells grown on flexible polymer films, Nature Materials 10 (2011) 857–861. https://doi.org/10.1038/NMAT3122

[8] L. L. Kazmerski, M. Hallerdt, P. J. Ireland, R. A. Mickelsen, and W. S. Chen, Optical properties and grain boundary effects in CuInSe2, Journal of Vacuum Science & Technology A: Vacuum, Surfaces, and Films 1 (1983) 395-398. https://doi.org/10.1116/1.571928

[9] E. Ghorbani, J. Kiss, H. Mirhosseini, G. Roma, M. Schmidt, J. Windeln, T. D. Ku¨hne, and C. Felser, Hybrid-functional calculations on the incorporation of Na and K impurities into the CuInSe2 and CuIn5Se8 solar-cell materials, The Journal of Physical Chemistry C 119 (2015) 25197–25203. https://doi.org/10.1021/acs.jpcc.5b07639

[10] S. H. Wei, S. B. Zhang, and A. Zunger, Effects of Ga Addition to CuInSe2 on its Electronic, Structural, and Defect Properties, Applied Physics Letters 72 (1998) 3199-3201. https://doi.org/10.1063/1.121548

[11] C. H. Huang, Effects of Ga Content on Cu(In,Ga)Se2 Solar Cells Studied by Numerical Modelling, Journal of Physics and Chemistry of Solids 69 (2008) 330-334. https://doi.org/10.1016/j.jpcs.2007.07.093

[12] M. Gloeckler, and J. R. Sites, Band-gap grading in Cu (In, Ga) Se2 solar cells, Journal of Physics and Chemistry of Solids 66 (2005) 1891-1894. https://doi.org/10.1016/j.jpcs.2005.09.087

[13] I. Repins, M. A. Contreras, M. Romero, Y. Yan, W. Metzger, J. Li, S. Johnston, B. Egaas, C. DeHart, and J. Schar, Characterization of 19.9% efficient CIGS absorbers. 33rd IEEE Photovoltaic Specialists Conference, San Diego, California, (2008) 1–6. https://doi.org/10.1109/PVSC.2008.4922628

[14] A. Chirilă, P. Reinhard, F. Pianezzi, P. Bloesch, A. R.Uhl, C. Fella, L. Kranz, D. Keller, C. Gretener, H. Hagendorfer, D. Jaeger, R. Erni, S. Nishiwaki, S. Buecheler, and A. N. Tiwari, Potassium-induced surface modification of Cu (In, Ga) Se 2 thin films for high-efficiency solar cells. Nature materials, 12(12) (2013) 1107-1111, DOI:10.1038/nmat3789

[15] M. A. Green, K. Emery, Y. Hishikawa, W. Warta, E.D. Dunlop, D.H. Levi, and A. W. Y. Ho-Baillie, Solar cell efficiency tables (version 49), Progress in photovoltaics: research and applications 25 (2017) 3-13. https://doi.org/10.1002/pip.2855

[16] P. Jackson, R. Wuerz, D. Hariskos, E. Lotter, W. Witte, and M. Powalla, Effects of heavy alkali elements in Cu (In, Ga) Se2 solar cells with efficiencies up to 22.6%, physica status solidi (RRL)–Rapid Research Letters 10 (2016) 583-586. https://doi.org/10.1002/pssr.201600199

[17] T. Kato, J. Wu, Y. Hirai, H. Sugimoto, and V. Bermudez, Record efficiency for thin-film polycrystalline solar cells up to 22.9% achieved by Cs-treated Cu (In, Ga)(Se, S) 2, IEEE Journal of Photovoltaics 9 (2019) 325-330. https://doi.org/10.1109/JPHOTOV.2018.2882206

[18] W. Jyh-Lih, H. Yoshiaki, K. Takuya, S. Hiroki, and B. Veronica, New World Record Efficiency up to 22.9% for Cu(In,Ga)(Se,S)2 Thin-Film Solar Cells, 7th World Conference on Photovoltaic Energy Conversion, Waikoloa, Hawaii, USA, (2018) 10-15.

[19] H. Movla, Optimization of the CIGS based thin film solar cells: Numerical simulation and analysis. Optik 125 (2014) 67-70. https://doi.org/10.1016/j.ijleo.2013.06.034

[20] M. Fathi, M. Abderrezek, F. Djahli, and M. Ayad, Study of thin film solar cells in high temperature condition, Energy Procedia 74 (2015) 1410-1417. https://doi.org/10.1016/j.egypro.2015.07.788

[21] P. Chelvanathan, M. I. Hossain, and N. Amin, Performance analysis of copper–indium–gallium–diselenide (CIGS) solar cells with various buffer layers by SCAPS, Current Applied Physics 10 (2010) S387-S391. https://doi.org/10.1016/j.cap.2010.02.018

[22] A. Benmir, and M. S. Aida, Analytical modeling and simulation of CIGS solar cells, Energy Procedia 36 (2013) 618-627. https://doi.org/10.1016/j.egypro.2013.07.071

[23] S. Dabbabi, T. B. Nasr, and N. Kamoun-Turki, Parameters optimization of CIGS solar cell using 2D physical modeling, Results in Physics 7 (2017) 4020-4024. https://doi.org/10.1016/j.rinp.2017.06.057

[24] H. Heriche, Z. Rouabah, and N. Bouarissa, High-efficiency CIGS solar cells with optimization of layers thickness and doping, Optik 127 (2016) 11751-11757.

[25] M. Abderrezek, M. Fathi, and F. Djahli, Comparative Study of Temperature Effect on Thin Film Solar Cells, Journal of Nano- and Electronic Physics 10 (2018) 02027. https://doi.org/10.21272/jnep.10(2).02027

[26] M. Mostefaoui, H. Mazari, S. Khelifi, A. Bouraiou, and R. Dabou, Simulation of high efficiency CIGS solar cells with SCAPS-1D software, Energy Procedia 74 (2015) 736-744. https://doi.org/10.1016/j.egypro.2015.07.809

[27] Atlas User's Manual. SILVACO Inc., Santa Clara, CA 95054, California, USA, 2018.

[28] S. M. Sze, and K. K. Ng, Physics of Semiconductor Devices, 3rd Ed, John Wiley & Sons, New Jersey, 2007.

[29] B. V. Van Zeghbroeck, Principles of Semiconductor Devices and Heterojunctions, Prentice Hall PTR, New Jersey, 2007.

[30] G. Hanna, A. Jasenek, U. Rau, and H. W. Schock, Influence of the Ga-content on the bulk defect densities of Cu (In, Ga) Se2, Thin Solid Films 387 (2001) 71-73. https://doi.org/10.1016/S0040-6090(00)01710-7.

[31] S. H. Song, K. Nagaich, E. S. Aydil, R. Feist, R. Haley, and S. A. Campbell, Structure optimization for a high efficiency CIGS solar cell, 35th IEEE Photovoltaic Specialists Conference, IEEE (2010) 002488-002492. https://doi.org/10.1109/PVSC.2010.5614724

[32] P. D. Paulson, R. W. Birkmire, and W. N. Shafarman, Optical characterization of CuIn1_x GaxSe2 alloy thin films by spectroscopic ellipsometry, Journal of Applied Physics 94 (2003) 879–888. https://doi.org/10.1063/1.1581345

[33] R. E. Treharne, A. Seymour-Pierce, K. Durose, K. Hutchings, S. Roncallo, and D. Lane, Optical design and fabrication of fully sputtered CdTe/CdS solar cells, Journal of Physics: Conference Series 286 (2011) 012038. https://doi.org/10.1088/1742-6596/286/1/012038

[34] M. Zeman, R. Swaaij, and J. Metselaar, Optical modeling of a-Si:H solar cells with rough interfaces: Effect of back contact and interface roughness, Journal of Applied Physics 88 (2000) 6436-6443. https://doi.org/10.1063/1.1324690

[35] M. A. Gloeckler, L. Fahrenbruch, and J. R. Sites, Numerical modeling of CIGS and CdTe solar cells: setting the baseline, 3rd World Conference on Photovoltaic Energy Conversion, IEEE (2003) 491-494. https://doi.org/10.1109/WCPEC.2003.1305328

[36] M. A. Gloeckler, Device Physics of Cu(In, Ga)Se2 Thin-Film Solar Cells, Ph.D. dissertation, Colorado State University, Fort Collins, USA, 2005.

[37] C. Larez, C. Bellabarba, and C. Rincon, Allow composition and temperature dependence of the fundamental absorption edge in CuGaxIn1-xSe2, Applied physics letters 65 (1994) 1650-1652. https://doi.org/10.1063/1.112944

[38] F. Grubišić-Čabo, S.Nižetić, and T. Giuseppe Marco, Photovoltaic panels: A review of the cooling techniques, Transactions of FAMENA, 40 (2016) 63-74.

[39] R. Stropnik, and U. Stritih, Increasing the efficiency of PV panel with the use of PCM, Renewable Energy 97 (2016) 671-679. https://doi.org/10.1016/j.renene.2016.06.011